Reactor Fuel Element Heat Conduction
via
Numerical Laplace Transform Inversion

Barry D. Ganapol and Roberto Furfaro[+]

Abstract. A newly developed numerical Laplace transform inversion (NLTI) will be presented to determine the transient temperature distribution within a nuclear reactor fuel element. The NLTI considered in this presentation has evolved to its present state over the past 10 years of application. The methodology adopted is one that relies on acceleration of the convergence of an infinite series towards its limit. The inversion will be applied to the prediction of the transient temperature distribution within an MTR type nuclear fuel element through a novel formulation of the solution to the transformed heat conduction equation.

1. Introduction. Laplace transforms and their inversions provide a valuable learning tool when demonstrating solutions to ordinary linear differential equations. The simplest and most efficient inversion, of course, is through table lookup or analytical continuation into the complex plane. However, complex analysis and table lookup do not always lead to the inversions sought. For numerical evaluation, it then may become necessary to apply a numerical Laplace transform inversion (NLTI), usually requiring some artful manipulation to enable the inversion. There are many numerical inversions on the market from which to choose all with at least one adjustable parameter that must be predetermined in order to generate reliable results. Numerical algorithms based on inverting an integral equation, taking limits of high order derivatives, various expansions of the integrand on the Bromwich contour and numerical quadrature of different flavors, are some of the various methods that have previously been proposed. In this presentation, a new inversion based on direct numerical integration on the Bromwich contour definition of the inversion integral will be presented and applied to determine the transient temperature distribution within the fuel element of an MTR type reactor.

a. Motivation for the LTI:R NLTI Algorithm

The numerical inversion is based on the Bromwich inversion integral defined as follows for $0 < t < \infty$:

$$f(t) = \frac{1}{2\pi i}\int_{g-i\infty}^{g+i\infty} ds e^{st}\overline{f}(s)$$

where g is to the right of the rightmost singularity of the image function $\overline{f}(s)$ given by

$$\overline{f}(s) \equiv \int_0^\infty dt e^{-st} f(t) \ .$$

Thus, analytical continuation into the complex s-plane is avoided by paying the penalty of treating highly oscillatory integrands. Our analysis will demonstrate the applicability of the proposed algorithm applied to image functions about which little information concerning the distribution of singularities is known.

[+]Department of Aerospace and Mechanical Engineering, University of Arizona, AME Bldg., 1130 N. Mountain Ave, Tucson AZ, 85721, USA ganapol@cowboy.ame.arizona.edu

The existence of so many numerical Laplace transform inversion algorithms, is an indication of the highly ill-conditioned nature of the inversion process. As has been shown [Davies and Martin, 1979], there are particular classes of functions for which certain algorithms give reliable results. Most of the algorithms developed to date have a tunable parameter that must be set within a particular interval in order to get the "best" results. Here the term "best" may refer to the fewest function evaluations or to the minimum error for a fixed number of function evaluations or just getting a numerical result at all. In many cases, the numerical procedure comes in two parts, i.e., a parameter determination based on a desired error and maximum machine precision and then the actual application of the numerical inversion algorithm itself. The present investigation encompasses a new line of reasoning that is based on the following observations:

1) No single NLTI algorithm is suitable for all classes of functions for all values of *t*.
2) Meaningful physical results are usually acceptable for a relative error in the range of 10^{-7} to 10^{-4}.
3) Computational effort is relatively unimportant in lieu of obtaining a reliable numerical result.
4) Computational effort is relatively inexpensive in today's computational environment.
5) A reliable NLTI algorithm should be able to generate results with minimum information known about the image function.

The NLTI presented in the following section has evolved to its present state over the past 10 years of application. The methodology adopted is one that relies on acceleration of the convergence of an infinite series towards its limit. This is a necessary feature of the algorithm, called **LTI:R** for Laplace transform inversion with Romberg integration, in order to resolve integrals with highly oscillatory integrands. As the name suggests, the usual trapezoidal integration employed in many inversion algorithms is replaced by a Romberg rule with a modest increase in computational effort. Finally, the choice of the Bromwich contour is determined by a minimization of the number of function evaluations as will be discussed.

b. Reactor Transient Heat Transfer Application

The **LTI:R** algorithm will be applied to an alternating fuel element/moderator reactor design in the 1-D plane approximation. For simplicity, a fixed cosine fission source will be assumed within each fuel element. A future publication will couple the neutron diffusion approximation directly to the heat conduction equation to provide a more realistic model. A helium gas moderator is assumed. The **LTI:R** algorithm has been applied to the heat conduction equations in a heterogeneous medium of more than 20 regions. This application represents an NTLI imbedded within a numerical procedure rather than for an explicit image function.

2. The LTI:R Algorithm

a. The Inversion Formula

The algorithm to be developed takes advantage of the following cosine integral form of the Laplace transform:

$$f(t) = \frac{2e^{gt}}{pt} \int_0^\infty dw \, \mathrm{Re}\, \overline{f}\left(g + i\frac{w}{t} \right) \cos(w) \, . \tag{1}$$

As suggested by many previous inversion algorithms [Davies and Martin, 1979], the approach of decomposing the cosine integral into integrals over the cosine periods will be followed to give

$$f(t) = \frac{2e^{gt}}{pt} \sum_{k=0}^{\infty} (-1)^k \int_0^p dw \, \mathrm{Re}\, \overline{f}\left(g + i\frac{w + kp}{t} \right) \cos(w) \, . \tag{2}$$

Each integration is performed using the Romberg integration rule featuring the re-use of function values. If

$$g(w) \equiv \mathrm{Re}\, \overline{f}\left(g + i\frac{w + kp}{t} \right),$$

the Romberg rule is

$$T_l^{m+1} = T_l^m + \frac{T_l^m - T_{l-1}^m}{4^{m+1} - 1} \, , \tag{3a}$$

initiated by the trapezoidal rule

$$T_l^0 = \frac{1}{2} T_{l-1}^0 + \frac{p}{2^l} \sum_{j=1,odd}^{2^l - 1} g\left(\frac{jp}{2^l} \right), \qquad T_0^0 = \frac{p}{2} \left[g(0) + g(p) \right] . \tag{3b}$$

The central feature of the algorithm will be acceleration of the convergence of the series in Eq.(2) using the nonlinear Wynn-epsilon acceleration [Baker and Graves-Morris, 1996]. The proposed algorithm is made possible only through the efficiency of convergence provided by the epsilon convergence accelerator.

b. Error Control

As with any numerical algorithm, its truth lies in the details of implementation. For the **LTI:R** algorithm, four potential sources of error have been identified.

b.1 Numerical quadrature error

The diagonal elements of the tableau formed by the Romberg approximations T_l^m are monitored for convergence using the relative error between two successive approximations

$$e_{R1} \equiv \left| \frac{T_l^{m+1} - T_l^m}{T_l^{m+1}} \right| \, . \tag{4}$$

In addition, the relative error between trapezoidal quadratures,

$$e_{R2} \equiv \left| \frac{T_{l+1}^0 - T_l^0}{T_{l+1}^{m+1}} \right| \, , \tag{5}$$

is also monitored for convergence. The integration is considered converged when $\min(e_{R1}, e_{R2}) \le e$ where e is the desired relative error for the inversion under consideration. In parallel, the trapezoidal integrations and the diagonal elements are considered sequences in *l* and *m* respectively. The epsilon algorithm is applied to each

sequence and e_{R2} and e_{R1} are replaced by the errors associated with the epsilon algorithm if smaller.

b.2 Wynn-epsilon algorithm

The Wynn-epsilon algorithm for the convergence of a sequence tending to a limit can be written as

$$\begin{aligned} e_{-1}^{(n)} &= 0,\ e_{0}^{(n)} = S_n \\ e_{k+1}^{(n)} &= e_{k}^{(n+1)} + \left[e_{k}^{(n+1)} - e_{k}^{(n)}\right]^{-1} \end{aligned} \tag{6}$$

where S_n is the sequence to be accelerated toward convergence. A tableau can be constructed with sequential diagonal elements interrogated for convergence. It could happen that the denominator of the second term in Eq.(6) vanishes leading to erroneous results. This situation is flagged and reported and since exact convergence has been achieved, either $e_{k}^{(n+1)}$ or $e_{k}^{(n)}$ is assumed to be the converged result. In the normal mode of operation, the final diagonal element of the tableau is returned as the limit to the sequence.

b.3 Loss of significance

When summing a series of numbers, there is always the potential for contamination by roundoff. In an attempt to minimize this contamination, the series in Eq.(2) is summed using compensated summation. After the sum is predicted to have converged after *n* terms and if the condition number

$$r \equiv \frac{\sum_{k=1}^{n} |a_k|}{\left|\sum_{k=1}^{n} a_k\right|}$$

is larger than $1/e$, then potential roundoff error has occurred. In this case, the relative integration error is continually reduced by a factor of 10 and the summation repeated until either no roundoff error is predicted or the integration tolerance is below machine accuracy. If the sum cannot be computed without roundoff, an error is indicated.

b.4 Series truncation error

The final source of error concerns the truncation of the series in Eq.(2). Here the error is estimated by

$$e_s \equiv \left|\frac{S_n - S_{n-1}}{S_n}\right| . \tag{7}$$

where S_n is either the epsilon algorithm result or original partial sum after *n* terms. The epsilon algorithm tableau is created using all partial sums less than or equal to *n*. The series is considered converged when $e_s \le e$ for two consecutive partial sums.

c. Numerical Implementation

c.1 Positioning of the Bromwich contour

Not unlike essentially all existing numerical Laplace transform algorithms, there is at least one parameter that needs to be predetermined in order for the **LTI:R** algorithm to operate properly. For the present case, the position g of the Bromwich contour on the real line needs to be specified. While, in theory, g need only be larger than the largest singularity, in practice, the numerical evaluation can be extremely sensitive to g. For this reason, special attention must be given to the choice of g to ensure reliable results.

Based on [Weideman, 1999], an optimization approach will be followed. The optimization, however, will not be based on the minimization of an error estimate since an explicit error estimate for the **LTI:R** algorithm is difficult to obtain because of the inclusion of the epsilon algorithm. Instead, an optimization will be based on the minimization of the number of function evaluations. Using the **BRENT** minimization routine [Press, et.,al., 1992] and assuming an initial g and a computational error of a factor of 10 times the desired error e, g is determined to give a local minimum number of function evaluations for a given t. This is done in order to minimize the computational time. Special attention must be taken to avoid an estimate of g that is less than the real part of the rightmost singularity. While the minimum found might not be a global minimum of the number of function evaluations, it is hoped that the g found will allow the inversion to proceed. However, at this point in the evaluation, there is no guarantee that the inversion obtained is accurate. To provide a sense of accuracy, the error is decreased by a factor of 10 (to e) and the inversion redone. This procedure is continued until either the relative error between two successive approximations is less than the desired error or e has been reduced to machine accuracy at which time an error diagnostic message is issued. The implementation of this error check is accomplished by re-using all previous function evaluations for each subsequent determination. In this way, the total computation time is reduced.

3. Demonstration

All calculations to be presented have been performed on a SUN Ultra 5 workstation for a desired relative error of 10^{-4}. The initial contour guess for all optimizations is $g = 10$.

a. Incorporation of LTI:R into a Numerical Procedure

While it is necessary for any numerical Laplace transform inversion to treat explicitly given image functions, a more useful demonstration of reliability is when the image function is not specified in closed form. Such a demonstration can be conceived of when the inversion is part of a numerical application. The demonstration to follow is intended to show that the **LTI:R** algorithm can be used confidently to analyze heat transfer in a highly heterogeneous material.

a.1 Transient heat transfer in an MTR fuel element

We now consider one-dimensional heat transfer in a heterogeneous slab configuration of an MTR fuel element of alternating fuel and moderator as shown in Fig.1.

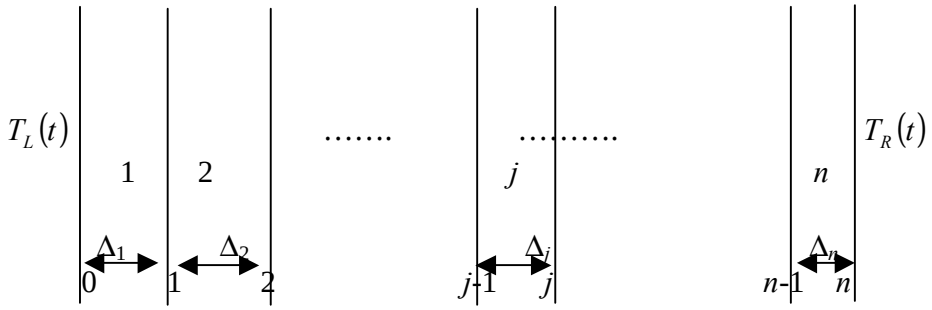

Fig.1 Reactor fuel configuration to be considered

The exterior wall temperatures are to vary according to a prescribed time variation and each slab can have a fixed fission heat source q(x) with a time variation of $r_0(t)$. The heat conduction equation

$$\frac{\partial w_j(x,t)}{\partial t} = k_j \frac{\partial^2 w_j(x,t)}{\partial x^2} + q(x) r_0(t) \tag{8a}$$

is to be solved in each material subject to the following external surface and initial conditions:

$$\begin{aligned} &w_0(0,t) = T_L(t), \quad w_n(x_n,t) = T_R(t) \\ &w_j(x,0) = T_{0j}(x). \end{aligned} \tag{8b}$$

The initial temperature distribution, $T_{0j}(x)$, is assumed to be the steady state distribution with inner and outer surface temperatures $T_L(0)$ and $T_R(0)$ respectively. For convenience, the spatial coordinate is measured in units of the square root of the average density times specific heat ($r_j C_j$) of each region. Since the initial steady state temperature distribution is assumed to satisfy

$$\begin{aligned} &\frac{d^2 T_{0j}(x)}{dx^2} = 0 \\ &T_{00}(x) = T_L(0) \\ &T_{0n}(x) = T_R(0), \end{aligned} \tag{9}$$

Eqs.(8) can be reformulated to eliminate the initial temperature distribution with the substitution

$$w_j(x,t) = T_{0j}(x) + u_j(x,t) \tag{10}$$

to give

$$\frac{\partial u_j(x,t)}{\partial t} = k_j \frac{\partial^2 u_j(x,t)}{\partial x^2} + q(x) r_0(t) \tag{11a}$$

$$\begin{aligned} &u_0(0,t) = T_L(t) - T_L(0), \quad u_n(x_n,t) = T_R(t) - T_R(0) \\ &u_j(x,0) = 0. \end{aligned} \tag{11b}$$

For completeness, the initial temperature distribution $T_{0j}(x)$ can be found without sources to be

$$T_{0j}(x)=\left[\frac{x-x_{j-1}}{\Delta_j}\right]T_{0j}+\left[1-\frac{x-x_{j-1}}{\Delta_j}\right]T_{0j-1} \tag{12a}$$

where T_{0j} are the interfacial temperatures satisfying the recurrence relation

$$T_{0j}-\left[1+\frac{\Delta_j k_{j-1}}{\Delta_{j-1}k_j}\right]T_{0j-1}+\left[\frac{\Delta_j k_{j-1}}{\Delta_{j-1}k_j}\right]T_{0j-2}=0\ . \tag{12b}$$

The solution for u_j will be obtained by first applying a Laplace transform in time to Eqs.(11) to give the coupled set of ODEs

$$\frac{d^2\bar{u}_j(x,s)}{dx^2}-\frac{s}{k_j}\bar{u}_j(x,s)=\frac{q(x)}{k_j}\bar{r}_0(s),\ 1\le j\le n \tag{13a}$$

with continuity of both temperature and heat flux at the material interfaces for $2 \le j \le n$-1

$$\begin{aligned}&\bar{u}_{j-1}(x_{j-1},s)=\bar{u}_j(x_{j-1},s)\\ &k_{j-1}\left.\frac{d\bar{u}_{j-1}(x,s)}{dx}\right|_{x=x_{j-1}}=k_j\left.\frac{d\bar{u}_j(x,s)}{dx}\right|_{x=x_{j-1}}\ .\end{aligned} \tag{13b}$$

The exposed surface conditions become

$$\begin{aligned}&\bar{u}_0(0,s)=\bar{T}_L(s)-T_L(0)/s\\ &\bar{u}_n(x_n,s)=T_R(s)-T_R(0)/s\ .\end{aligned}$$

For a fission source of the form

$$q(x)=q_{0j}\cos\left(b_j\left(x-\bar{x}_j\right)\right)$$

with $b_j\equiv p/\Delta_j$ and $\bar{x}_j\equiv\left(x_j+x_{j-1}\right)/2$ in region *j*, the most mathematically convenient solution to Eqs.(13) is of the form

$$\begin{aligned}\bar{u}_j(x,s)=\frac{1}{S_j}\Bigg[&\sinh\left(\frac{\sqrt{s}}{\sqrt{k_j}}\left(x_j-x\right)\right)\bar{u}_{j-1}(s)+\sinh\left(\frac{\sqrt{s}}{\sqrt{k_j}}\left(x-x_{j-1}\right)\right)\bar{u}_j(s)\Bigg]+\\ &+q_{0j}\cos\left(b_j\left(x-\bar{x}_j\right)\right)\bar{r}_0(s)/\left(s+k_j b_j^{\,2}\right)\end{aligned} \tag{14}$$

where

$$S_j\equiv\sinh\left(\frac{\sqrt{s}}{\sqrt{k_j}}\Delta_j\right)$$

and $\bar{u}_j(s)$ are the transforms of the interfacial temperature rises yet to be determined. From a substitution of the solution into the interfacial conditions, the following recurrence relation results:

$$\begin{aligned}&\bar{u}_j(s)+b_j(s)\bar{u}_{j-1}(s)+a_j(s)\bar{u}_{j-2}(s)=g_j\\ &\bar{u}_0(s)=\bar{T}_L(s)-T_L(0)/s\\ &\bar{u}_n(s)=\bar{T}_R(s)-T_R(0)/s\end{aligned} \tag{15}$$

where the coefficients are known in terms of the thermal conductivities and g_j in terms of source parameters.

For the source free case, where the inner wall temperature rise is to be kept at zero for all t [$\bar{u}_0(s) = 0$], the solution to the 3-point recurrence relation above can be expressed as

$$\bar{u}_j(s) = \left[\frac{e_j(s)}{e_n(s)}\right]\left[\bar{T}_R(s) - T_R(0)/s\right] \tag{16a}$$

where

$$\begin{aligned} &e_j(s) + b_j(s)e_{j-1}(s) + a_j(s)e_{j-2}(s) = 0 \\ &e_0 = 0, \;\; e_1 = 1\,. \end{aligned} \tag{16b}$$

This recurrence is solved by reduction to a two point nonlinear recurrence to avoid instability. The general solution of Eq.(15) can be constructed from superposition of recurrences for left and right boundary conditions and the source. The alternative solution for $\bar{u}_j(s)$ is by matrix inversion which, while costly, is generally required for a large number of slabs since the inhomogeneous source recurrence may become unstable.

The numerical inversion, therefore, consists of the determination of $\bar{u}_j(s)$ recursively and then the inversion of Eq.(14) for the spatial/temporal temperature increment. Thus, this application offers a suitable test of **LTI:R** where the image function is only numerically available.

Figure 2 shows a heatup test of the reactor fuel element (without a fission source) with 5 fuel plates separated by helium gas. The temperature on the right boundary of the fuel element is increased from zero to one exponentially [$1 - e^{-t}$] while the temperature on the left boundary is held at zero. The approach to the linear steady state temperature distribution is clearly apparent. The temperature in the fuel is nearly constant with a large rise in temperature in the helium coolant as anticipated. Figure 3 shows the trend toward steady state as the fission source is introduced exponentially [$r_0(t) = 1 - e^{-10t}$]. Because of the relatively large fuel thermal conductivity, the fuel temperature at steady state will be nearly uniform with the primary temperature drop in the coolant.

References

[1] Baker, G.A. and Graves-Morris, P. R, *Padé Approximants*, Cambridge University Press, 1996.

[2] Davies, B. and Martin, B., *J. Comp. Phys*., 33(1979), 1-32.

[3] Press, W.H., Vettering, W.T., Teulolsky, S.A., Flannery, B.P., *Numerical Recipes*, Cambridge University Press, 1992.

[4] Weideman, J.A.C., *SIAM J. Sci. Comput*.,21, 1999, 111-128.

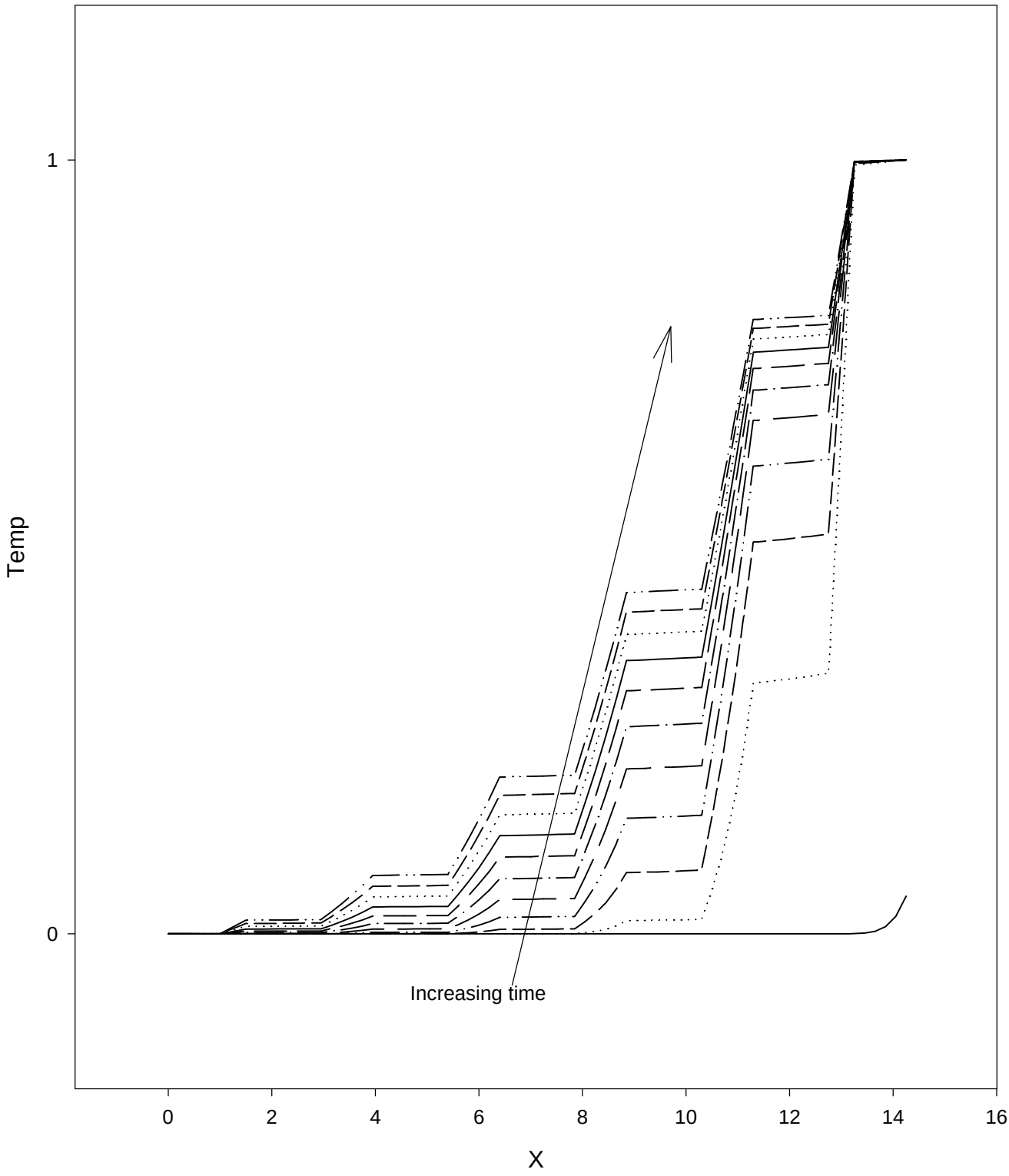

Fig. 2 Approach to steady state for MTR fuel element heatup test

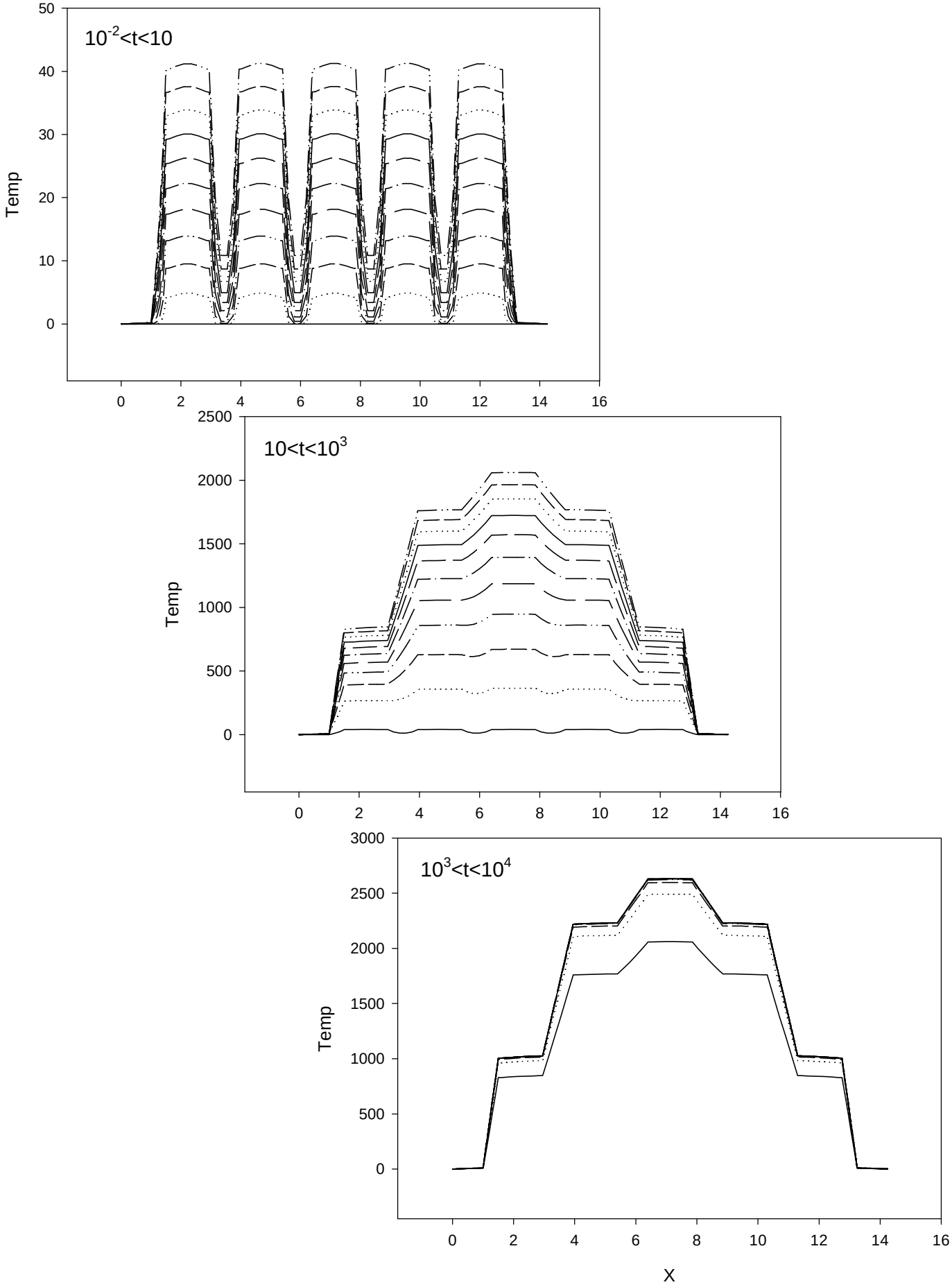

Fig. 3 Evolution toward steady state of MTR fuel element